



ELSEVIER

Journal of Alloys and Compounds 330–332 (2002) 132–140

Journal of
ALLOYS
AND COMPOUNDS

www.elsevier.com/locate/jallcom

Short hydrogen–hydrogen separations in novel intermetallic hydrides, $\text{RE}_3\text{Ni}_3\text{In}_3\text{D}_4$ (RE=La, Ce and Nd)

V.A. Yartys^{a,*}, R.V. Denys^b, B.C. Hauback^a, H. Fjellvåg^c, I.I. Bulyk^b, A.B. Riabov^b,
Ya.M. Kalychak^d

^aInstitute for Energy Technology, P.O. Box 40, N-2027 Kjeller, Norway

^bKarpenko Physico-Mechanical Institute, National Academy of Sciences of Ukraine, 5, Naukova Str., Lviv 290601, Ukraine

^cDepartment of Chemistry, University of Oslo, N-0315 Oslo, Norway

^dDepartment of Chemistry, Lviv State University, 6, Kyryla and Mefodiya Str., Lviv 79005, Ukraine

Abstract

Crystal structure data for deuterides RENiInD_x (RE=La, Ce and Nd) are provided on the basis of high-resolution powder X-ray and neutron diffraction data. The materials retain the hexagonal ZrNiAl type structure on deuteration. The formation of saturated deuterides is connected with anisotropic expansion along [001]. In the saturated hydrides, $\text{RE}_3\text{Ni}_3\text{In}_3\text{D}_4$, hydrogen atoms are located inside RE_3Ni tetrahedra that share a common face, thereby forming a RE_3Ni_2 trigonal bipyramid. This results in extraordinary short H–H separations of around 1.6 Å. This feature is unique among well characterised metal hydride materials and is in striking contrast with the generally obeyed empirical rule of 2.0 Å for H–H separations. On heating, the saturated materials release half of their hydrogen content at low temperatures, thereby statistically filling just one out of the two neighbouring tetrahedra. The remaining, more strongly bonded hydrogen, is released below 500°C under dynamic vacuum. © 2002 Elsevier Science B.V. All rights reserved.

Keywords: Hydrides; Powder neutron diffraction; Lanthanum; Cerium; Neodymium; Nickel; Indium

1. Introduction

The atomic separation between hydrogen atoms that fill interstices in the metal sublattice of a metal hydride, is ruled by repulsive H···H interactions, which in practice is assumed to prevent any further enclosure than 2.0 Å. This observation is valid for a vast number of well-characterised metal hydrides and is generalised as the empirical ‘rule of 2 Å’ [1,2].

Metal–hydrogen systems with H–H separations significantly shorter than 2 Å have not been reported so far. Actually, there are early reports on D–D distances of 1.79 Å in Th_2AlD_4 [3], however, a recent high-resolution powder neutron diffraction study shows that the correct distance is 1.97 Å [4]. On the other hand, there exist metal complexes where dihydrogen H_2 is coordinated to the transition metal. For some of these, the H–H bond is elongated from 0.74 Å in molecular H_2 to around 0.82 Å [5]. In such complexes it is more and more evident that the

H–H distances may span the range from 0.74 Å to more than 1.5 Å dependent on the character of the bonding (from dihydrogen to hydride) [5].

The ZrNiAl type structure of ABC intermetallics is found for many aluminides [6]. By substituting Al atoms with larger In atoms for RE-based compounds, the *ab*-plane of the hexagonal structure expands. This makes hydrogen absorption more favourable owing to enlarged interstitial sites. In RENiIn compounds different sites have been considered for hydrogen absorption, e.g. tetrahedral RE_2NiIn sites [7]. The structure contains furthermore face-sharing RE_3Ni tetrahedra that form a RE_3Ni_2 trigonal bipyramid. However, the filling of such tetrahedral sites with H-atoms has been considered unlikely on the basis of the ‘rule of 2 Å’ [7]. The present study actually shows that this is feasible, however, one thereby obtains unusually short H–H separations that are unique among known metal hydrides.

The present paper describes synthesis and thermal stability of RENiIn -deuterides, RE=La, Ce and Nd. Emphasis is put on describing the relationship between composition, unit cell deformation, hydrogen site occupa-

*Corresponding author. Tel.: +47-63-806-453; fax: +47-63-812-905.
E-mail address: volodymyr.yartys@ife.no (V.A. Yartys).

tion and unusually short H–H interatomic separations with basis in high-resolution powder X-ray (synchrotron) and neutron diffraction data. Since the findings are of extraordinary character, special attention is given to the analysis of the diffraction data in order to rule out any uncertainty or chance for misinterpretation.

2. Experimental

Alloys with stoichiometric composition RENiIn were prepared from high purity elements (rare earth metals (La, Ce, Nd), nickel and indium; all 99.9% or better) by arc melting in argon atmosphere. The samples were thereafter annealed in vacuum at 600°C for 4 weeks, before being quenched into ice water. Powder X-ray diffraction analysis indicated a formation of phase pure RENiIn samples that crystallise with the hexagonal ZrNiAl-type structure (see Fig. 1 as representative example). The unit cell dimensions of the RENiIn phases were determined from powder X-ray diffraction data and were in good agreement with reference data [6].

Deuteration of the RENiIn compounds was performed at room temperature and gas pressures 0.1–0.5 MPa (D_2 purity 99.8%). In all cases deuterium absorption resulted in formation of RENiIn $D_{1.3}$ deuterides.

Crystal structure data for the deuterides were derived on the basis of different sets of powder diffraction data. Conventional, high-resolution XRD data were collected with a Siemens D5000 diffractometer (Cu $K\alpha_1$ radiation; primary monochromator, PSD detector; sample in transmission mode). Synchrotron (SR) powder XRD data were measured at the Swiss–Norwegian Beam Lines at ESRF, Grenoble ($\lambda=0.49868$ Å, channel cut primary monochromator, secondary Si(111) analyser, cylinder geometry). Powder neutron diffraction (PND) data were collected with the PUS two-axis instrument (JEEP II reactor, Kjeller;

$\lambda=1.5550$ Å). Measurements at 7 K were performed by means of a Displex cooling system. For the SR and PND measurements, the samples were kept in sealed 0.3-mm diameter glass capillaries and sealed 5-mm diameter vanadium cans, respectively. Crystal structure data were derived by Rietveld (profile) refinements using one or more of the collected data sets and the GSAS program [8].

Comparative analysis of the diffraction profiles for the intermetallic alloys and corresponding deuterides showed no evidence of peak widening or peak splitting after hydrogenation. Furthermore, since there is no difference in halfwidths between the 002 and $hk0$ reflections of the hexagonal structure (see Fig. 2 as example), it is unlikely that deuteration leads to lowering of the crystal symmetry.

In accordance with earlier findings for RENiIn– H_2 [7], complete deuterium absorption is accompanied by anisotropic expansion of the unit cell along [001]. Since no extra peaks appear in neither the XRD nor PND patterns, any hexagonal superstructure formation (e.g. with $a=n \cdot a_{\text{hex}}$; $c=m \cdot c_{\text{hex}}$) can be ruled out. For ‘lower’ deuterides RENiIn $D_{0.67-x}$ the unit cell data are consistent with previous observations for RENiIn– H_2 : the deuterides remain hexagonal but with a small expansion of both a_{hex} and c_{hex} with respect to RENiIn.

After syntheses, the RENiIn $D_{1.3-x}$ samples were handled in an Ar-filled glove box and transferred from the autoclaves into vanadium sample holders which thereafter were sealed with indium washers. The PND studies showed that no significant deuterium desorption had taken place for LaNiIn $D_{1.3-x}$ and CeNiIn $D_{1.3-x}$ during such handling, and the PND data corresponded to nearly single phase deuterides. The Nd-containing deuteride has lower thermal stability and partial deuterium desorption took place in the glove box. This desorption resulted in a two-phase mixture of the higher deuteride, NdNiIn $D_{1.3-x}$ (87 wt%) and the lower deuteride, NdNiIn $D_{0.55}$ (13 wt%).

Special attention was paid to sample quality for the

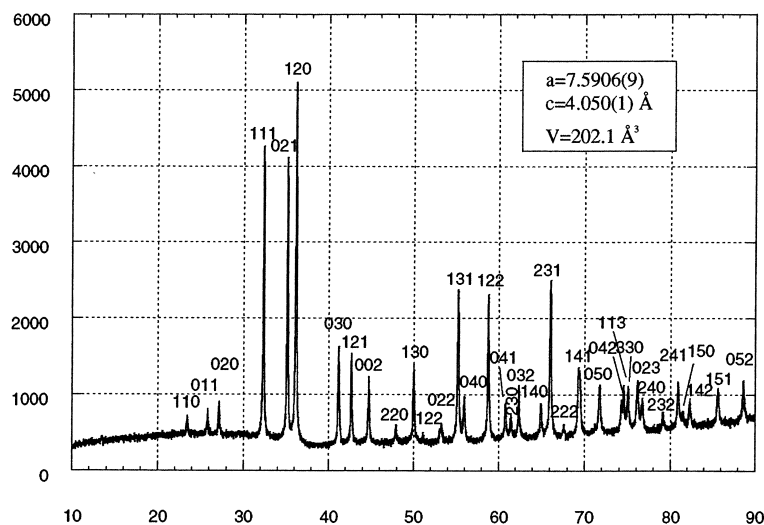


Fig. 1. PXD profile for the LaNiIn intermetallic compound (Siemens D5000 diffractometer, Cu $K\alpha_1$ radiation).

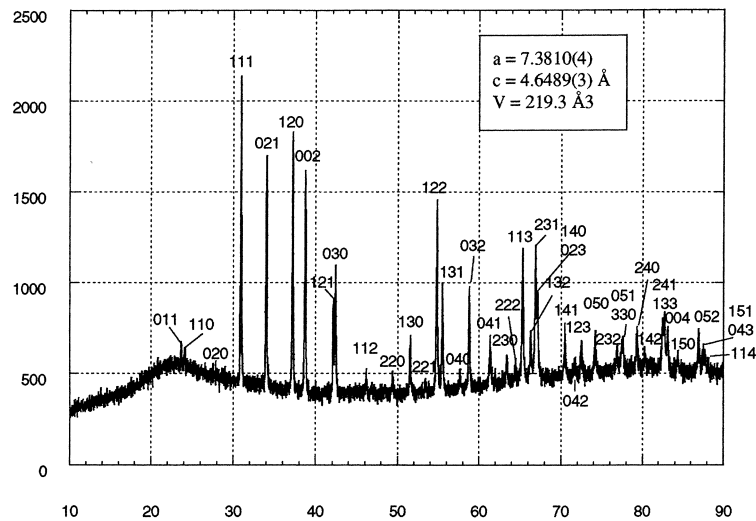


Fig. 2. PXD profile for the $\text{LaNiInD}_{1.3}$ deuteride (Siemens D5000 diffractometer, $\text{Cu K}\alpha_1$ radiation).

'lower' deuterides $\text{LaNiInD}_{0.67-x}$, $\text{CeNiInD}_{0.67-x}$ and $\text{NdNiInD}_{0.55}$ prior to PND data collection, i.e. the samples are achieved free of $(\text{La,Ce,Nd})\text{NiInD}_{1.3-x}$ impurities. The 'lower' deuterides were obtained from $\text{RENiInD}_{1.3-x}$ by applying vacuum desorption in secondary vacuum after heating the samples slowly ($1-2^\circ/\text{min}$) until the desired annealing temperature. These temperatures were 220°C (La), 185°C (Ce) and 190°C (Nd). The samples were annealed until no further significant D desorption was observed (12 h at maximum). The structure data derived for $\text{NdNiInD}_{0.55}$ were used in the refinements of the diffraction data for the higher deuteride $\text{NdNiInD}_{1.3-x}$.

During the refinements of the PND data the background

was modelled as a cosine Fourier series polynomial. No diffuse scattering contributions were observed that would be indicative of major short range order (see patterns in Figs. 3 and 4). The same situation was found for $\text{NdNiInD}_{1.3-x}$, which was studied both at 298 and at 7 K. The lack of liquid-like background behaviour over the whole temperature range was taken as a strong indication for D-ordering.

The Rietveld analysis (space group $P\bar{6}2m$) showed unequivocally that deuterium atoms occupy a single crystallographic site ($4h$) located on the 3-fold axis of the RE_3Ni tetrahedron. All other tetrahedral interstices in the RENiIn structure, including $12l_1$, $12l_2$, $6j_1$, $6j_2$ (all

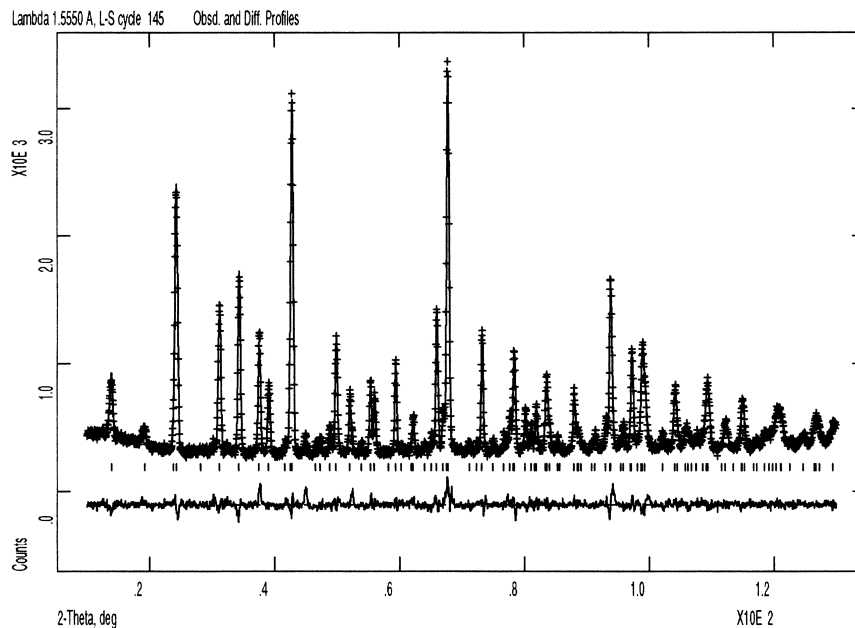


Fig. 3. Observed (+), calculated (upper line) and difference (lower line) high-resolution powder neutron diffraction profiles for $\text{LaNiInD}_{1.22}$ collected with the PUS instrument ($\lambda = 1.5550 \text{ \AA}$). Positions of peaks are marked.

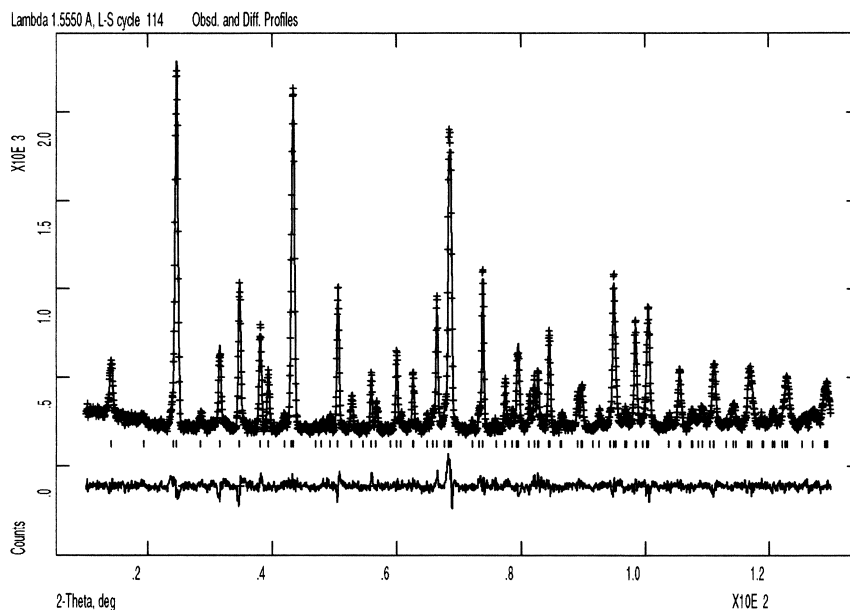


Fig. 4. Observed (+), calculated (upper line) and difference (lower line) high-resolution powder neutron diffraction profiles for $\text{CeNiInD}_{1.24}$ collected with the PUS instrument ($\lambda = 1.5550 \text{ \AA}$). Positions of peaks are marked.

RE_2NiIn), $3f$ (Nd_2In_2) and $6i$ (NdNiIn_2) sites are empty (consult Ref. [7] for detailed description of sites). During these refinements, the following parameters were varied: one overall scale factor, five peak profile parameters (modelled by a mixed Gaussian–Lorentzian function), two unit cell dimensions, three positional parameters (one for each of RE, In, D), occupation factor for D and five isotropic temperature factors. Altogether 2400 data points and 93–100 Bragg reflections, depending on the unit cell parameters of deuteride, were included in the least squares refinements.

For $\text{RE}=\text{Nd}$, a few additional parameters were refined owing to the two phase situation: (a) mass ratio between $\text{NdNiInD}_{1.3-x}$ and $\text{NdNiInD}_{0.55}$; (b) structural parameters for $\text{NdNiInD}_{0.55}$ including two unit cell constants, three positional parameters and one occupation factor (five isotropic temperature factors were fixed). Note that independently of the complexity of the samples (single phase for $\text{LaNiInD}_{1.3-x}$ and $\text{CeNiInD}_{1.3-x}$ or two-phase for $\text{NdNiInD}_{1.3-x}$) the crystal structure data for all compounds were found to be in excellent mutual agreement.

No constraints were introduced during the refinements. No significant correlations between the deuterium occupancy and the temperature factors that would influence the D/RENiIn ratios were observed. The derived value for $U_{\text{iso}}(\text{D})$ corresponds to that typically found for metal hydrides at 298 K, and for $\text{NdNiInD}_{1.2}$ also at 7 K.

The obtained fit between observed and calculated intensities is excellent, in particular when keeping the low number of free atomic coordinates (three) in mind. Nevertheless, the finding of very short H–H separations along [001] called for special considerations of possible symmetry lowering or local displacements. Splitting of the D site

into three equivalent sites by displacements away from the 3-fold axis, gave immediately inferior reliability factors. Likewise, anisotropic description of the deuterium displacement parameters did not give any significant improvement in the fit nor any indications for a non-spherical tensor. The lack of such features in the 7 K low temperature data is considered as an important proof of D-atoms being located in the $4h$ sites.

The thermal stability of the deuterides was studied with use of the thermal desorption spectroscopy technique. The samples were heated in secondary vacuum at a heating rate of 5 K/min.

3. Results and discussion

The hexagonal ZrNiAl type structure taken by the RENiIn compounds can formally be considered as a layered structure with a repeated stacking of two different planar nets of compositions RE_3Ni_2 and In_3Ni along [001] of the hexagonal unit cell (see Fig. 5). Modest deuteration levels ($z < 0.67$; RENiInD_z) leads to a rather isotropic expansion of the unit cell (see Table 1). On further absorption and formation of the saturated (0.1 MPa D_2 pressure) $\text{RENiInD}_{1.3-x}$ deuterides, the chemically induced lattice expansion is strongly anisotropic. Despite huge expansion along [001] ($\Delta c/c = 14.8\text{--}16.5\%$), Rietveld analysis of high-resolution SR-XRD data shows that the structural deformation does not lead to any substantial rearrangement of the metal atoms within the planar nets. None of these atoms are significantly shifted in x , y coordinates from those of the intermetallic RENiIn . The volume expansion on hydrogenation amounts to maximum

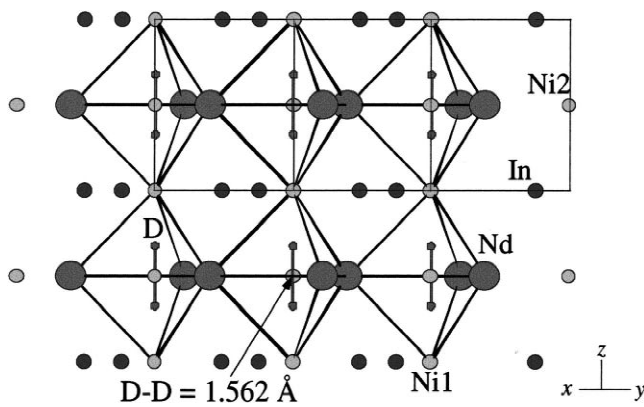


Fig. 5. Crystal structure of NdNiInD_{1.19} showing different 'layers' along [001] and the short D–D separations.

7.5–9.0% which is rather moderate. Actually, the huge interlayer expansion is accompanied by a smaller intralayer contraction ($\Delta a/a = -(2.8\text{--}3.9)\%$). The volume increment per absorbed D atoms is significant; $4.1\text{--}4.7 \text{ \AA}^3/\text{at.D}$. The unit cell parameters a , c and V decrease as expected for the intermetallic compounds and their (saturated) deuterides from RE=La via Ce to Nd.

Unit cell data and interatomic distances as obtained from Rietveld refinements of the PND data are summarised in Tables 1 and 2. Reliability factors of the refinements are given in Table 3, and atomic coordinates in Table 4. The RENiInD_{1.3–x} deuterides (RE=La, Ce, Nd) are all isostructural and D atoms fill equivalent interstitial sites between the layers. The ideal, fully saturated deuterides have composition RE₃Ni₃In₃D₄ (RENiInD_{1.33}). For the present samples the occupancy of the interlayer D sites exceeds 90%. The deuterium atoms are coordinated by RE₃Ni tetrahedra. However, owing to the RE₃Ni₂–In₃Ni stacking sequence, such tetrahedra share a common RE₃ triangular face and form a trigonal bipyramid (TB) which is doubly occupied by deuterium, see Fig. 5. As a consequence, D–D pairs are formed in the structure with

Table 1

Unit cell and chemical expansion data for RENiInD_{1.3–x} (RE=La, Ce, Nd) as derived from powder neutron diffraction data at 298 K

	a (Å)	$\Delta a/a$ (%)	c (Å)	$\Delta c/c$ (%)	V (Å ³)	$\Delta V/V$ (%)	$\Delta V/\text{at.D}$ (Å ³)
LaNiIn	7.5906(9)		4.050(1)		202.08		
LaNiInD _{0.48}	7.7004(8)	1.45	4.0733(5)	0.58	209.17	3.51	4.93
LaNiInD _{1.22}	7.3810(4)	–2.76	4.6489(3)	14.8	219.33	8.54	4.69
CeNiIn	7.534(1)		3.975(1)		195.39		
CeNiInD _{0.48}	7.5919(3)	0.77	3.9947(2)	0.50	199.40	2.05	2.77
CeNiInD _{1.24}	7.2921(3)	–3.21	4.6238(2)	16.3	212.93	8.98	4.73
NdNiIn	7.5202(8)		3.9278(8)		192.37		
NdNiInD _{0.55}	7.593(1)	0.97	3.9916(9)	1.62	199.30	3.60	4.20
NdNiInD _{1.19}	7.2255(4)	–3.92	4.5752(3)	16.5	206.85	7.53	4.05
NdNiInD _{0.54} ^a	7.562(1)	n.a.	3.987(1)	n.a.	197.44	n.a.	n.a.
NdNiInD _{1.23} ^a	7.1954(4)	n.a.	4.5716(3)	n.a.	204.97	n.a.	n.a.

Calculated standard deviations in parentheses.

^a $T = 7$ K.

Table 2

Interatomic distances for RENiInD_{1.3–x} and RENiInD_{0.67–x} (RE=La, Ce, Nd) as derived from powder neutron diffraction data at 298 K

	RE–D (Å)	Ni–D (Å)	D–D (Å)
LaNiInD _{0.48}	2.362(4)	1.68(1)	>3 ^b
LaNiInD _{1.22}	2.407(2)	1.507(4)	1.635(8)
CeNiInD _{0.48}	2.319(3)	1.694(6)	>3 ^b
CeNiInD _{1.24}	2.371(2)	1.509(3)	1.606(6)
NdNiInD _{0.55}	2.297(8)	1.71(4)	>3 ^b
NdNiInD _{1.19}	2.342(2)	1.506(9)	1.562(9)
NdNiInD _{0.54} ^a	2.296(7)	1.70(4)	>3 ^b
NdNiInD _{1.23} ^a	2.337(2)	1.501(4)	1.570(8)

Calculated standard deviations in parentheses.

^a $T = 7$ K.

^b The distances between the 'split', less than 50% occupied, sites are: 0.71(3) Å [LaNiInD_{0.48}], 0.61(1) Å [CeNiInD_{0.48}], 0.56(8) Å [NdNiInD_{0.55} at 298 K] and 0.59(7) Å [NdNiInD_{0.54} at 7 K].

Table 3

Reliability factors for Rietveld refinements of powder neutron and powder X-ray diffraction data at 298 K

	PND			XRD		
	R_{pr}	R_{wpr}	CHI^2	R_{pr}	R_{wpr}	CHI^2
LaNiIn	4.41	5.23	1.17			
LaNiInD _{0.48}	5.31	6.74	1.11			
LaNiInD _{1.22}	4.34	5.72	1.54			
CeNiInD _{0.48}	5.22	6.66	1.20	4.48	6.32	2.96
CeNiInD _{1.24}	4.96	6.40	1.33			
NdNiInD _{0.55}	4.14	5.29	1.37			
NdNiInD _{1.19}	4.29	5.48	1.35	3.70	5.08	2.34
NdNiInD _{1.23} ^a	3.82	4.89	1.28			

^a $T = 7$ K.

extremely short interatomic separations of around 1.6 Å. The fits of the powder XRD and PND data are shown for NdNiInD_{1.3–x} in Figs. 6–8.

The length of the c -axis of the fully deuterated RE₃Ni₃In₃D₄ samples is determined by the linear Ni–

Table 4

Atomic coordinates^a and U_{iso} (10^{-2} \AA^2) derived from Rietveld refinements of powder neutron diffraction data

	LaNiInD _{0.48} 298 K	LaNiInD _{1.22} 298 K	CeNiInD _{0.48} 298 K	CeNiInD _{1.24} 298 K	NdNiInD _{0.54} 298 K	NdNiInD _{1.19} 298 K	NdNiInD _{0.55} 7 K	NdNiInD _{1.23} 7 K
RE in 3g x	0.593(1)	0.6035(4)	0.5914(11)	0.6013(6)	0.582(3)	0.6004(5)	0.586(3)	0.6011(5)
U_{iso}	1.4(2)	0.6(1)	1.5(1)	0.8(1)	1.0(–)	0.51(8)	0.1(–)	0.1(–)
Ni1 in 2c U_{iso}	2.2(2)	1.3(1)	1.7(1)	1.13(6)	1.0(–)	1.15(7)	0.2(–)	0.1(–)
Ni2 in 1b U_{iso}	1.6(2)	1.1(1)	1.7(1)	1.14(7)	1.0(–)	1.02(8)	0.2(–)	0.25(8)
In in 3f x	0.242(2)	0.2437(7)	0.2479(11)	0.2462(6)	0.251(4)	0.2476(7)	0.250(5)	0.2480(7)
U_{iso}	0.9(2)	0.7(1)	1.0(1)	0.9(1)	1.0(–)	0.7(2)	0.5(–)	0.1(1)
D in 4h z	0.587(3)	0.6759(8)	0.576(1)	0.6737(7)	0.571(10)	0.6707(10)	0.574(9)	0.6717(8)
U_{iso}	1.7(4)	2.0(1)	0.7(2)	1.93(8)	2.0(–)	2.0(1)	0.2(–)	1.3(1)
Occupancy	0.36(1)	0.919(10)	0.362(6)	0.927(9)	0.41(3)	0.894(10)	0.41(3)	0.923(9)

Space group $P\bar{6}2m$ (No. 189). Calculated standard deviations in parentheses.^a Sites: 1b, 0,0,1/2; 2c, 1/3,2/3,0; 3f, x,0,0; 3g, x,0,1/2; and 4h, 1/3,2/3,z.

D···D–Ni chains, and equal $2d_{\text{Ni–D}} + d_{\text{D–D}}$. The Ni–D bond distances are nearly constant for the entire series: 1.507(4) Å (RE=La), 1.509(3) Å (RE=Ce) and 1.506(9) Å (RE=Nd), see Table 2. On the other hand, the D–D separations decrease gradually from 1.635(8) for La, via 1.606(6) for Ce to 1.562(9) Å for Nd. It is likely that this variation is a consequence of the shortening of the corresponding RE–Ni bonds.

The variation of the RE–D distances follows the same trend as found for the binary hydrides of the rare earth metals, i.e. the RE–D distance decreases from La to Nd; here being 2.407(2) Å (La), 2.371(2) Å (Ce) and 2.342(2) Å (Nd) (Table 2).

The La–D and Ni–D distances in LaNiInD_{1.3} are shorter than in LaNiD_{3.7} [9] and LaNiSnD₂ [10], i.e. structures where the D-atoms also occupy La₃Ni tetrahedra (see Table 5 for the details). At the same time, a significant shortening is evident for the La–La distances in the

structure of LaNiInD_{1.3}, not only in comparison with LaNiD_{3.7} and LaNiSnD₂, but also when compared to the LaNiIn intermetallic (Table 5). This may indicate that La–La bonds in LaNiInD_{1.3} can act as a shielding, or to some extent compensate, for the possibly repulsive interactions between close D atoms in the D···D pairs.

The thermal stability of the RENiInD_{1.3–x} deuterides is rather low taking into account that the D atoms are located in ‘attractive’ RE₃Ni interstitial positions. Fig. 9 shows that deuterium desorption starts slightly above room temperature. The main desorption event is at low temperatures, with peak at 110–115°C (RE=La and Ce) and <100°C (RE=Nd). For all RE this event is completed at around 200°C and leads to removal of approximately 50% of D and formation of RENiInD_{0.67–x} deuterides. The thermal stability of the RENiInD_{1.3–x} is similar to those for the chemically related TbNiAlH_{1.1} [11], where hydrogen removal also proceeds in a step-wise manner and starts

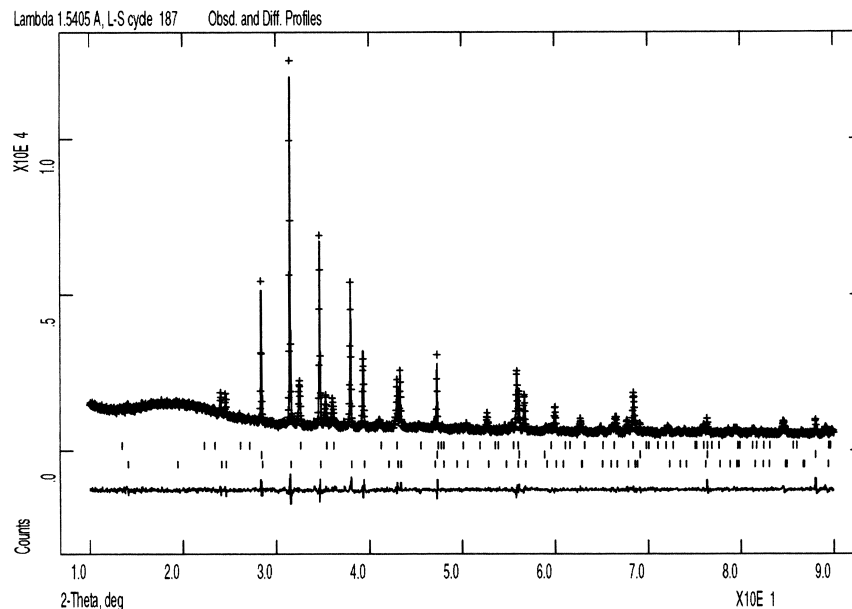


Fig. 6. Observed (+), calculated (upper line) and difference (lower line) high-resolution XRD profiles for NdNiInD_{1.19} collected with a D5000 instrument in transmission mode. Positions of peaks are marked; from bottom to top NdNiInD_{1.19}, Si standard and NdNiInD_{0.55}.

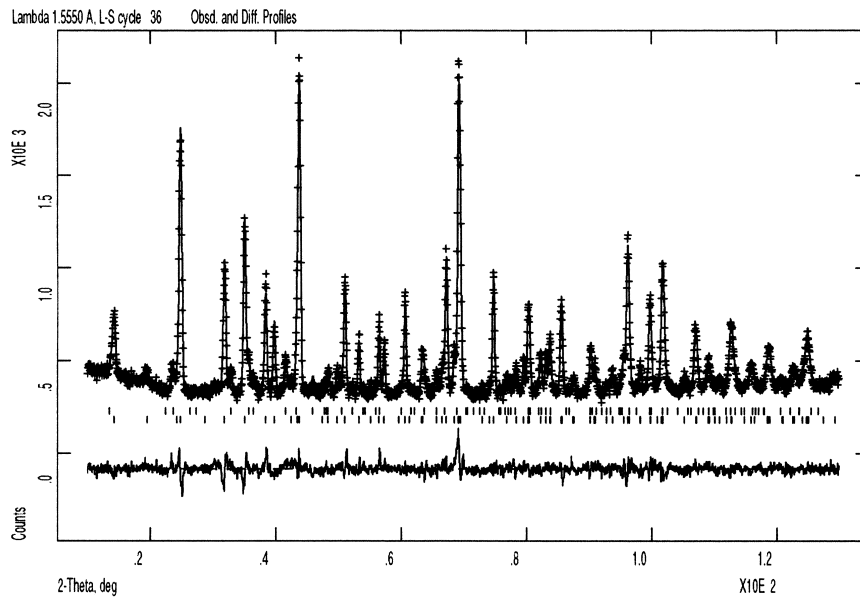


Fig. 7. Observed (+), calculated (upper line) and difference (lower line) high-resolution powder neutron diffraction profiles for $\text{NdNiInD}_{1.19}$ collected with the PUS instrument ($\lambda = 1.5550 \text{ \AA}$). Positions of peaks are marked; from bottom to top $\text{NdNiInD}_{1.19}$ and $\text{NdNiInD}_{0.55}$.

in the vicinity of room temperature. However, for $\text{TbNiAlH}_{1.4}$ the desorption occurs from Tb_2NiAl sites. These sites contain atoms of a *p*-element (Al) in their nearest surroundings and, thus, have a reduced bonding energy for the accommodated H. On the other hand, for LaNiSnD_2 the desorption occurs from La_3Ni sites; however, the thermal stability is around 200°C higher [10] than for $\text{RENiInD}_{1.3-x}$. This increase in stability correlates with a significantly larger size of the La_3Ni tetrahedra in

LaNiSnD_2 ($r = 0.69 \text{ \AA}$) than in $\text{LaNiInD}_{1.3}$ ($r = 0.47 \text{ \AA}$). Similar correlations between crystal structure and H desorption properties were reported previously for the deuterides of Zr_3FeD_x ($x = 1.3, 2.5$ and 5.0) [12,13] and $\text{Zr}_6\text{FeAl}_2\text{D}_x$ ($x = 5.6$ and 1.3) [14]. In both cases a close relation between the size and occupancy of the Zr_4 tetrahedra has been established [12–14].

The first step of deuterium desorption from $\text{RENiInD}_{1.3-x}$ corresponds to conversion of

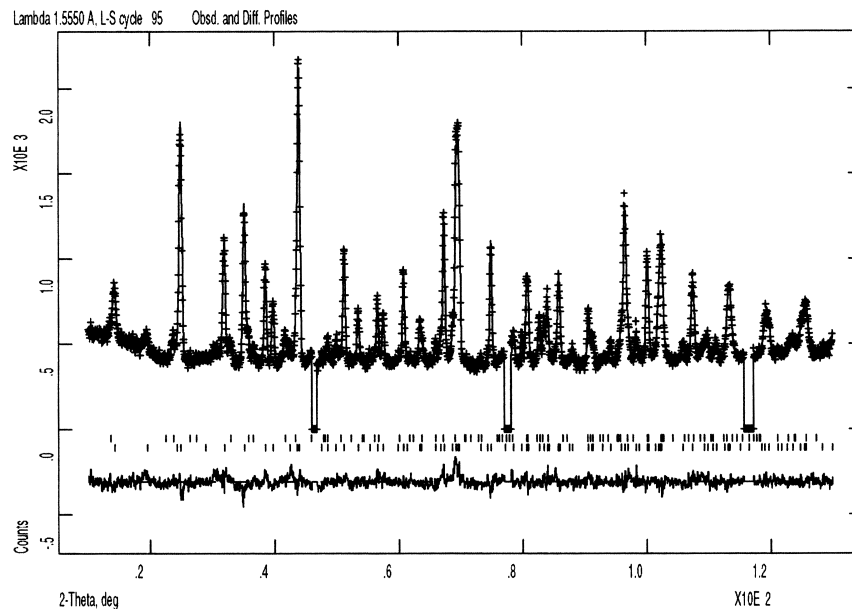


Fig. 8. Observed (+), calculated (upper line) and difference (lower line) high neutron diffraction profiles for $\text{NdNiInD}_{1.23}$ collected with the PUS instrument ($\lambda = 1.5550 \text{ \AA}$) at 7 K. Positions of peaks are marked; from bottom to top $\text{NdNiInD}_{1.23}$ and $\text{NdNiInD}_{0.54}$. Three intervals of 2θ are excluded owing to cryostat reflections.

Table 5

Interatomic distances (Å) in chemically similar La_3Ni tetrahedra occupied by atoms D in the structures of $\text{LaNiD}_{3.7}$, LaNiSnD_2 and $\text{LaNiInD}_{1.3}$ in comparison with LaNiIn

	La–La	La–Ni	La–D	Ni–D
$\text{LaNiD}_{3.7}$ [9]	3.980	2×3.199	2.409	1.727
	2×4.238	3.427	2×2.483	
LaNiSnD_2 [10]	3×4.422	3×3.350	3×2.612	1.618
$\text{LaNiInD}_{1.3}$ (this work)	3×3.921	3×3.245	3×2.407	1.507
LaNiIn (this work)	3×3.956	3×3.052	–	–

For comparison: $2r_{\text{La}} = 3.754$ Å; $r_{\text{La}} + r_{\text{Ni}} = 3.123$ Å.

$\text{RENiInD}_{1.19-1.24}$ into $\text{RENiInD}_{0.67-x}$. Deuterium atoms are thereby removed from at least half of the available RE_3Ni tetrahedra. On average, this converts the originally doubly occupied RE_3Ni_2 bipyramid into becoming singly occupied. However, the D atoms do not fill the trigonal bipyramidal sites but are (dynamically) positioned in one of the two neighbouring RE_3Ni tetrahedra (i.e. split positions).

For these lower $\text{RENiInD}_{0.67-x}$ deuterides, the unit cell expansion is isotropic and rather small relative to the initial alloy; $\Delta a/a = 0.77-1.45\%$, $\Delta c/c = 0.50-1.62\%$, $\Delta V/V = 2.1-3.6\%$ (Table 1). Again a , c and V decrease in the sequence La–Ce–Nd. The volume increments per absorbed D atom are less than in the saturated $\text{CeNiInD}_{1.24}$

for RE=Ce ($2.8 \text{ \AA}^3/\text{at.D}$), but roughly unchanged for RE=La and Nd (i.e. $4.2-4.9 \text{ \AA}^3/\text{at.D}$).

In the lower deuterides, the partly filled D sites are situated just $0.6-0.7 \text{ \AA}$ apart (Table 2). Since the site occupancy is less than one half, two neighbouring sites are most probably never simultaneously occupied. In practice this implies that the D···D separations in $\text{RENiInD}_{0.67-x}$ along [001] are >3 and $>4 \text{ \AA}$ in the basal plane. The refinements indicate for this average picture that Ni–D distances increase, being approximately $0.1-0.2 \text{ \AA}$ longer than in the saturated $\text{RENiInD}_{1.3-x}$. The D atoms remain significantly shifted away from the RE_3 face towards the Ni atom. The RE–D distances are slightly shorter for the lower deuterides than for saturated deuterides, being, respectively, $2.362(4) \text{ \AA}$ for RE=La, $2.319(3) \text{ \AA}$ for RE=Ce, and $2.297(8) \text{ \AA}$ for Nd.

The residual deuterium in the lower deuterides is strongly bonded to the metal sublattice in accordance with the favourable RE_3Ni tetrahedral sites. Its complete removal, providing reversible formation of the initial intermetallic RENiIn , takes place in vacuum at rather high temperatures, $300-500^\circ\text{C}$. On this basis it is tempting to suggest that the easy removal of the first deuterium from $\text{RENiInD}_{1.33}$ is due to gain in energy by removing D atoms from the face sharing tetrahedra.

Finally, we note that ^1H NMR of the RENiIn -based hydrides has given independent indications for the existence of H···H pairs in the compounds of Ce [15,16] and Pr [17]. On the basis of NMR data the H···H separations has been estimated to be equal to 1.48 \AA in CeNiInH_x [15] and $1.5-1.8 \text{ \AA}$ in PrNiInH_x [17]. Preliminary results from ongoing electronic structure calculations show that there is no H···H bonding interactions in $\text{La}_3\text{Ni}_3\text{In}_3\text{D}_4$ (P. Ravindran, personal communication, 2000).

In conclusion, the present study shows that a novel feature with close H-neighbours at distances of $1.562-1.635 \text{ \AA}$ occurs in the hexagonal structures of $\text{RENiInD}_{1.3-x}$ (RE=La, Ce, Nd). The H···H interaction is mediated via a triangular RE_3 cluster with probably strong RE···RE bonds, thus ‘shielding’ the direct H···H interaction. The present first observations of short H···H separations are in sharp contrast with the available crystal structure data for metal hydrides, where H···H separations are governed by the ‘rule of 2 \AA ’. Certainly, the most interesting and intriguing questions concerning the nature of the H···H interaction in the RENiIn -based hydrides is not yet answered and will undoubtedly be in focus in forthcoming studies.

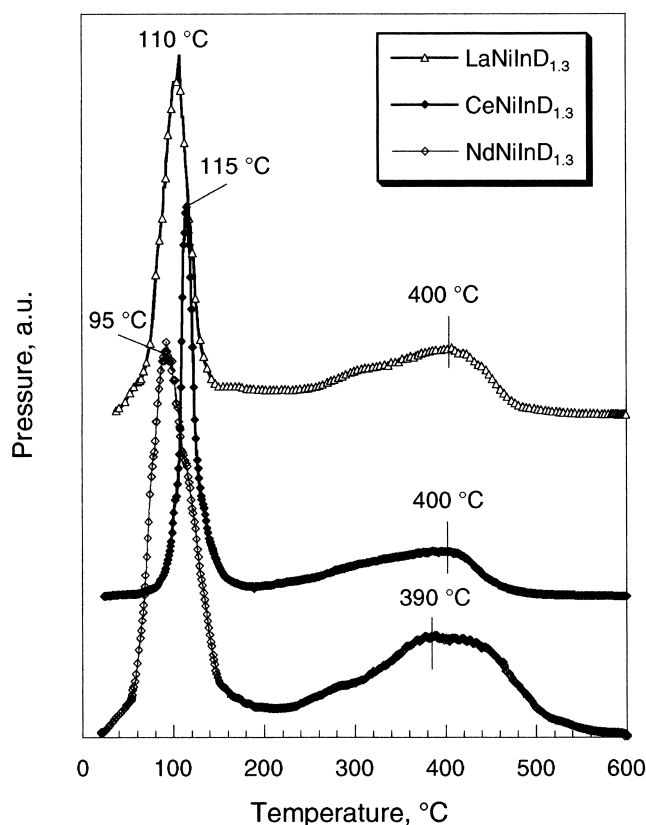


Fig. 9. Trace showing desorption of deuterium from $\text{RENiInD}_{1.3-x}$ (RE=La, Ce, Nd) deuterides under dynamical vacuum conditions.

Acknowledgements

We are grateful to Dr. V.I. Zaremba (Lviv University), M.H. Sørby (University of Oslo) and T. Olavesen (University of Oslo) for their assistance in experimental work

and to the Swiss Norwegian Beam Lines at ESRF for the possibility to collect high quality powder diffraction data.

References

- [1] D.G. Westlake, *J. Less-Common Met.* 75 (1980) 177.
- [2] A.C. Switendick, *Z. Phys. Chem. N.F.* 117 (1979) 89.
- [3] J. Bergsma, J.A. Goedkoop, *Acta Crystallogr.* 14 (1961) 223.
- [4] M.H. Sørby, H. Fjellvåg, B.C. Hauback, A.J. Maeland, V.A. Yartys, *J. Alloys Comp.* 309 (1–2) (2000) 154.
- [5] G.J. Kubas, *J. Less-Common Met.* 172–174 (1991) 475.
- [6] E.I. Hladyshevskiy, O.I. Bodak, in: *Crystal Chemistry of Inter-metallic Compounds of Rare Earth Metals*, Vyszczka Szkoła, Lviv, 1982, 254 pp.
- [7] I.I. Bulyk, V.A. Yartys, R.V. Denys, Ya.M. Kalychak, I.R. Harris, *J. Alloys Comp.* 284 (1–2) (1999) 256.
- [8] A.C. Larson, R.B. von Dreele. *General Structure Analysis System (GSAS)*, LANSCE, MS-H 805 (1994).
- [9] V.A. Yartys, V.V. Burnasheva, N.V. Fadeeva, S.P. Solov'ev, K.N. Semenenko, *Int. J. Hydrogen Energy* 7 (1982) 957.
- [10] V.A. Yartys, T. Olavesen, B.C. Hauback, H. Fjellvåg, H.W. Brinks, *J. Alloys Comp.* 330–332 (2002) 141.
- [11] V.A. Yartys, F. Gingl, K. Yvon, L.G. Akselrud, A.V. Kolomietz, L. Havela, T. Vogt, I.R. Harris, B.C. Hauback, *J. Alloys Comp.* 279 (2) (1998) L4.
- [12] V.A. Yartys, H. Fjellvåg, B.C. Hauback, A.B. Riabov, M.H. Sørby, *J. Alloys Comp.* 287 (1–2) (1999) 189.
- [13] V.A. Yartys, H. Fjellvåg, I.R. Harris, B.C. Hauback, A.B. Riabov, M.H. Sørby, I.Yu. Zavaliy, *J. Alloys Comp.* 293–295 (1999) 74.
- [14] V.A. Yartys, H. Fjellvåg, B.C. Hauback, *J. Alloys Comp.* 290 (1/2) (1999) 157.
- [15] K. Ghoshray, B. Bandyopadhyay, M. Sen, A. Ghoshray, N. Chatterjee, *Phys. Rev.* B47 (13) (1993) 8277.
- [16] M. Sen, S. Giri, K. Ghoshray, B. Bandyopadhyay, A. Ghoshray, N. Chatterjee, *Solid State Commun.* 89 (4) (1994) 327.
- [17] M. Sen, A. Ghoshray, K. Ghoshray, S. Sil, N. Chatterjee, *Phys. Rev.* B53 (21) (1996) 14345.